VACUUM INSULATION PANEL

VIPA

GLOBAL ASSOCIATION

An Advanced Technique for Measuring the Effect of Moisture Content on the Thermal Conductivity of Fumed Silica VIPs

A VIPA- Funded Project conducted by Dr Yoash Carmi and Eddie Shufer,

Avery Dennison Hanita, April 2017

Introduction

The degradation rate of VIPs depends not only on the permeation rate of the different atmospheric gases through the envelope, but also on the response of the core material to the increasing presence of these permeated gas molecules. Recent lab and field tests on fumed silica (FS) panels show that the degradation rate of FS panels is predominantly determined by the moisture permeating through the envelope, and much less by the permeating air molecules. Over the last two years Avery Dennison Hanita has developed a very efficient and easy-to-operate technique for measuring the response of any core material to the increasing pressure of air: - **the λvsP curve**. However, there is no easy-to-operate technique available for measuring the relation between the amount of moisture absorbed by FS cores and their thermal conductivity.

In this project, Avery Dennison Hanita faced this challenge by upgrading and modifying the λvsP technology to apply it to moisture content (MC), **the λvsMC curve**.

This newly developed technique can be used by labs for qualification of commercial panels and by labs and industrial companies to characterized newly developed core materials.

Background

Accurate prediction of the long-term performance of fumed silica panels is very important for creating reliable industrial standards for VIPs. It is also a significant factor in the development of new core materials, since the response to accumulated moisture has a huge effect on performance throughout their decades-long service life.

In the early 21st century, pioneering experimental work was made [1] to measure the dependence of the thermal conductivity of fumed silica samples by exposing the core to different levels of moisture, re-evacuating the panel and measuring its thermal conductivity by the guarded hot plate technique. The internal moisture vapor pressure was measured using the liftoff technique. Two of the most important results of the ZAE work are presented below. Figure 1 shows how the thermal conductivity of a 20mm thick fumed silica panel changes with moisture content levels at a mean temperature of 10^0C. The second figure presents the relation between the moisture content and the relative humidity inside the panel - the sorption isotherms curves.

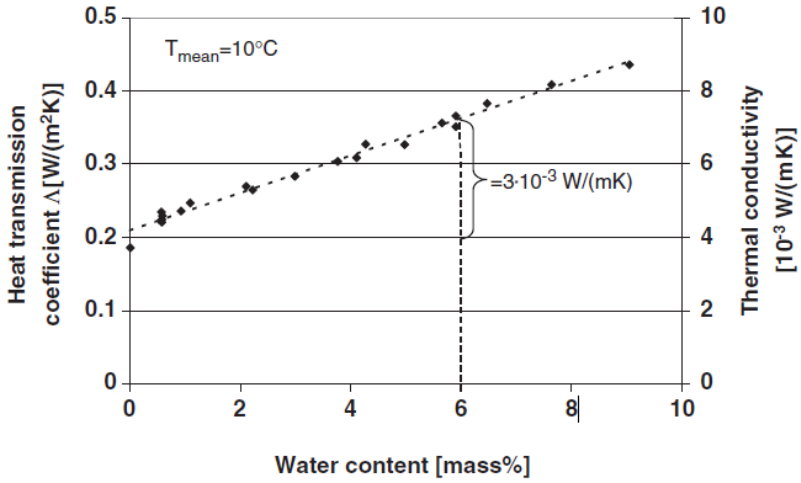

Heat transmission coefficient Λ (left) and thermal conductivity λ (right) depending on the water content X_w in 20-mm thick VIPs at a mean temperature of 10°C.

Figure 1

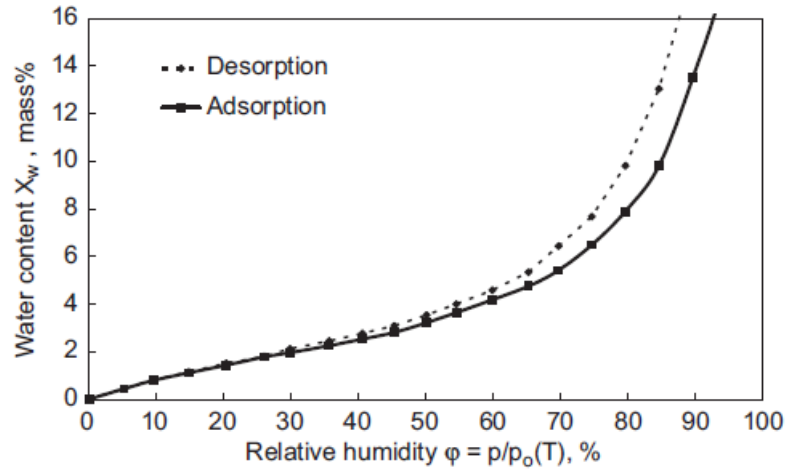

Sorption isotherms for fumed silica kernels at 23 °C. Plotted is the water content in mass% of the dry kernel versus the relative vapour pressure [20].

Figure 2

This report describes a new generation of measuring techniques that allows easier and faster procedures. In addition, no extra pressure measurement by the liftoff device is required. In the new technique, both the thermal conductivity and the pressure of the moisture vapor are measured simultaneously by a very accurate pressure gauge connected to the internal volume of the panels. One major drawback of the technique used by ZAE was that it took a very long time to get to steady-state moisture distribution inside the core after any change of the moisture content. With the new approach, the time to reach steady-state moisture distribution during the thermal conductivity measurement is substantially reduced.

During the project, the new measuring technique was applied to three types of fumed silica cores, providing a new understanding of the effect of moisture absorption on the thermal conductivity of the powders. In addition, important differences were found between the three cores.

Description of the New Measuring Technique

The newly proposed approach is based on the successful technique developed by Avery Dennison Hanita for measuring the λvs P curves of core materials, as shown in Figure 3 below. The core under testing is located at the left side of the envelope while a leak-tight connector is joins to the right side of the bag. The flat left side is used for measuring the thermal conductivity of the core while the connector on the right is used for evacuating the panel, accurately measuring the internal pressure using two pressure gauges. This allows a measured quantity of moisture through a vacuum valve mounted on one arm of the connector into the evacuated space for controlled changes of the moisture content of the core.

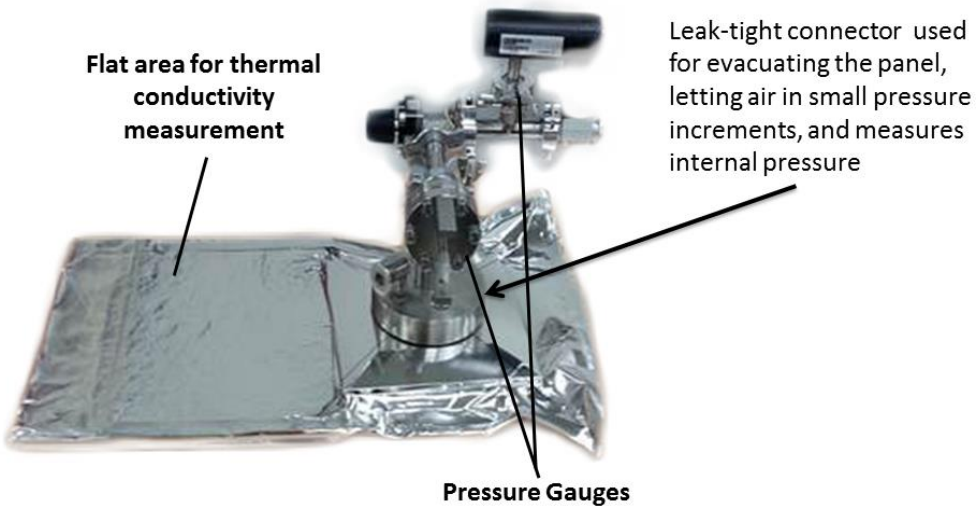

Figure 3

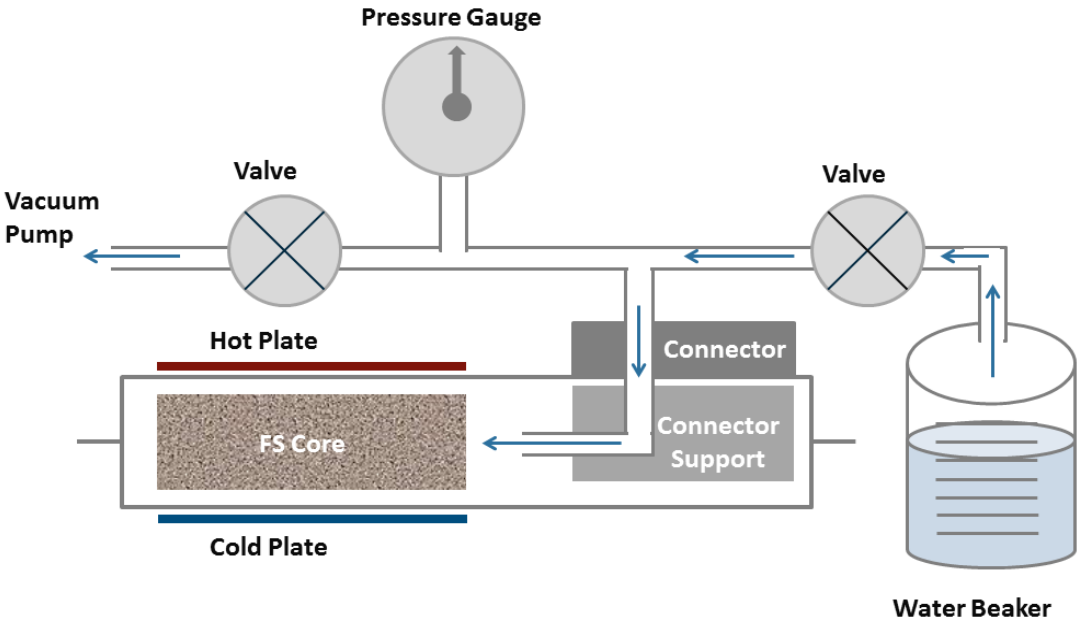

Figure 4 Drawing of the system for measuring the effect of moisture content on the thermal conductivity of the panel and on the pressure of the moisture vapor.

1. **Equipment used**
   a. LaserComp 314 heat flux λ machine
   b. Capacitive pressure gauges
   c. Turbo molecular pump
2. **Samples tested:**
   a. Three fumed silica panels provided by three different VIP manufactures, A, B, and C, were tested to determine their λvs Water Content curves.
   b. The capacity of one type of CaO and the water vapor pressure as a function of its water content were also measured.
3. **Description of the first test procedure**:
   A. **Sample preparation**: 300mm X 300mm X 15.4mm fumed silica core provided by manufacturer A was placed inside the bag of the system described above. The weight of the dry core was 257g (density 0.185g/cm3) and its thermal conductivity after a very long evacuation time was measured to be 4.9mW/mK. The temperature of the plates of the LaserComp λ machine was set to 2^0C and 18^0C (10^0C mean temperature). The part of the mVIP system containing the core material was kept for a few weeks between the plates of the λ machine for the entire duration of the test without changing the temperature setup. By doing so, the part with the core of the mVIP system

was kept under a constant temperature gradient created by the different temperatures of the plates. This ensured that the system was constantly very close to steady-state water distribution inside the core even when more water was inserted.

B. **Increasing the water content**: The leak-tight measuring glass tube (labelled water beaker in Figure 4 above) connected to the mVIP system was filled with 10cc of water, and all the air molecules above the water level were removed by the turbo molecular pump. After opening the system valves, a slow delivery of water vapor from the glass tubing into the core area started, caused by the pressure difference between the core area and the water vapor pressure built inside the glass tubing due to evaporation. Very important: The temperature of the entire piping system was kept higher than the glass tubing to avoid internal condensation. Hot air was used for heating the piping system.

C. **Water delivery rate:** Without heating the water measuring tube, about 1cc of water was delivered in 8 hours. This translates to a water content increase rate of about 0.046% per hour.

D. **Reaching steady-state:** During the nights, the valves were closed and the panel was kept between the two plates of the λ machine to reach steady-state distribution of the water molecules inside the panel. By analyzing the changes of the λ night-time readings we could see that constant λ values were measured after just a few hours. Presumably steady-state water concentration distribution inside the panel was achieved very quickly due to the slow delivery rate and especially because the slow process of increasing water content was carried out at a steady-state temperature gradient between the 2^0C cold plate and the 18^0C hot plate.

4. Results: The λvs Water content curve of the FS Core A

The graphs and the table below describe the dependence of the thermal conductivity of the panel made with the FS core provided by manufacturer A as a function of the water content at steady-state conditions with 2^0C on the cold side of the panel and 18^0C on the warm side.

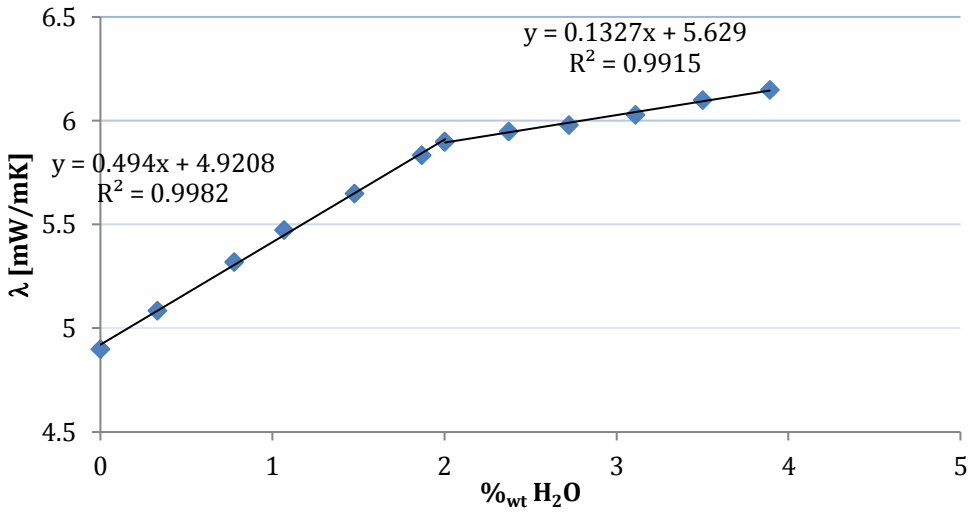

Figure 5.

The center of panel thermal conductivity of the fumed silica core provided by manufacturer A as function of the water content of the absorbed moisture. Till about 2% water content, the slope of the curve followed the results of the work [(1)] done by ZAE more than a decade ago. Above 2%, the added water probably condensed close or on the internal cold surface of the panels, causing a 3.7 times slower thermal conductivity increase rate.

H_2O [ML]	λ [MW/MK]	Δλ [MW/MK]	$\%_{WT}$ H_2O	Δλ / $\%_{WT}$ H_2O
0	4.9	0	0	
0.85	5.085	0.185	0.3307393	0.559352941
2	5.32	0.42	0.778210117	0.5397
2.75	5.475	0.575	1.070038911	0.537363636
3.8	5.65	0.75p	1.478599222	0.507236842
4.8	5.835	0.935	1.86770428	0.500614583
5.15	5.9	1	2.003891051	0.499029126
6.1	5.95	1.05	2.373540856	0.442377049
7	5.98	1.08	2.723735409	0.396514286
8	6.03	1.13	3.112840467	0.3630125
9	6.1	1.2	3.501945525	0.342666667
10	6.15	1.25	3.891050584	0.32125

Table 1

The measured data of λ as function of the water content taken on core A at steady-state conditions (2^0C-18^0C). The data points of the slope of the curve λvs Water content are shown in the far-right column.

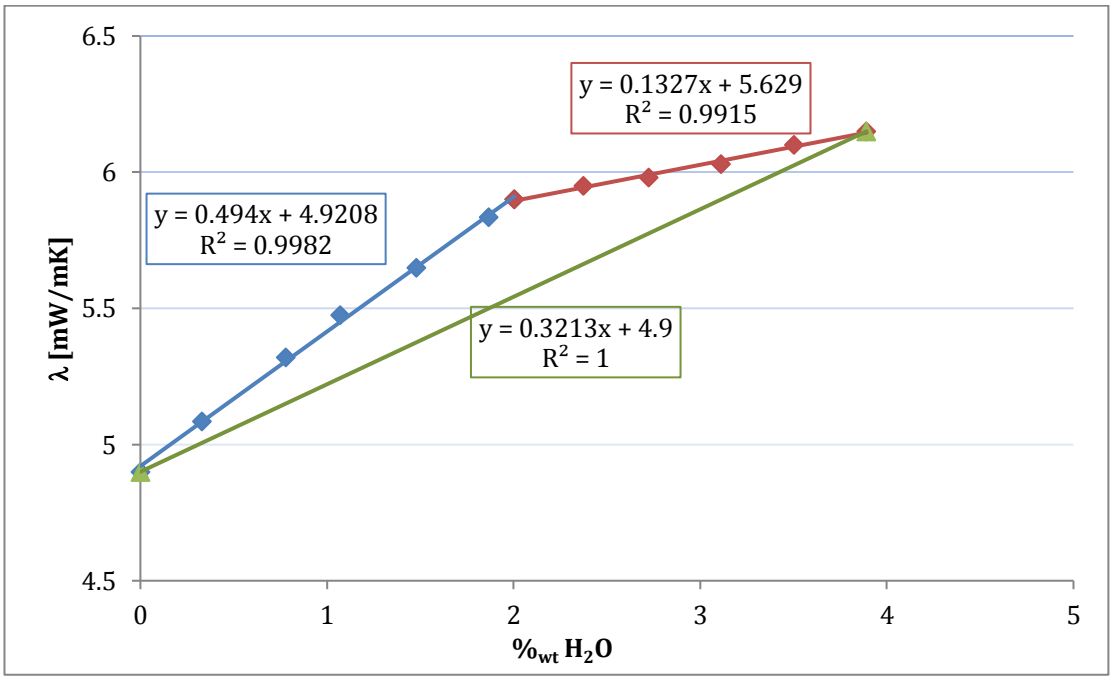

Figure 6

As in Figure.5, the center of panel thermal conductivity of the fumed silica core provided by manufacturer A as function of the water content of the absorbed moisture. The mean thermal conductivity increase rate up to 4% water content was 0.32(mW/mK)/1%.

5. Preliminary analysis of the investigation on core A

a. The technique described above for measuring the dependence of the thermal conductivity of fumed silica panels seems to work very well.

b. The first set of results closely agrees with the results of the measurements taken by ZAE(1) up to water content of about 2%.

c. Because of the temperature gradient inside the panel (2^0C-18^0C) at about 2% water content, the dew point is reached at the internal cold side of the panels.

d. Adding more water into the panel above 2% water content resulted in 3.7 times smaller thermal conductivity dependence on the water content.

e. Another interesting observation: adding more water into the panel (kept at 2^0C-18^0C) above 2% up to 4% did not alter the water vapor pressure inside the panel; it kept constant at about 8.5 mbar. This is another indication to the possibility that above 2%, water content condensation starts inside the panel.

6. Measuring the dependence of the thermal conductivity on the two temperatures of the plates of the λ machine.

a. After reaching 3.9% water content with core A, the dependence of the measured values of λ on the temperatures of the hot and the cold plates of the λ machine was also measured.
At plate temperatures of 2^0C-18^0C, the following steady-state values were measured: λ = 6.13mWmK, water vapor pressure P = 8.4mbar

At 10^0C – 35^0C: λ=6.54mW/mK, water vapor pressure P=14.8mbar.

These new results support the assumption that at a water content of 3.9%, large quantities of water condensed close to the cold plate. At higher temperatures, the water vapor which was at the saturation pressure at the temperature of the cold plate rose, causing more absorption by the core and an increase of the measured value of λ, in addition to the larger contribution by the IR radiation to the overall thermal conductivity.

7. Measuring the λvs Water content curve of the FS Core B

The same test procedure carried out on core A was also performed on a 19.4mm thick core provided by manufacturer B. The density of this core under vacuum was 0.182g/cm^3.

As before, the panel was placed between the two plates of the λ machine along the entire duration of the test with 2^0C on the cold plate and 18^0C on the hot one.

This time, in addition to measuring the increasing values of thermal conductivity, readings of the internal water vapor pressure were also taken. The data describing the evolution of the water vapor pressure along the test duration is shown in Table 4 in the Appendix below. With this 19.4mm thick core, the time required for reaching steady-state conditions was much longer compared to core A: a few days to one week were required to reach steady-state conditions. The λ data as function of the water content is shown in Table 2 and presented graphically also in Figure 2 where the λvs Water content curve for core B is plotted.

Core B responded quite differently from core A to the absorbed moisture:

a. The levelling off point of core B occurred at a lower water content level (1.5%) compared to core A (2%). At a higher moisture content than the level off point, the thermal conductivity of core B rose 2.75 faster than core A: 0.365mW/mK/1%, compared to 0.133mW/mK/1%.

b. As a result of 1 and 2, the average slope of core B (0.461{mW/mK}/1%) was found to be 1.44 times larger than for core A (0.321{mW/mK}/1%).

c. The time required to reach steady-state was much longer with core B (a few days to a week) compared to core A (a few hours). The 5mm additional thickness probably cannot explain this big difference. Presumably it is also related to specific properties of the two powders. More work should be done to find the reasons for this big variance in response to the absorbed moisture.

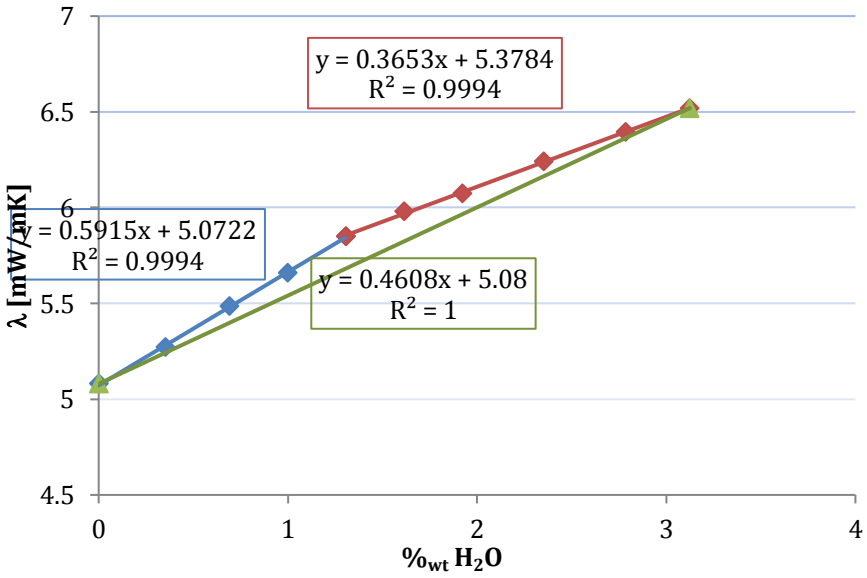

Figure 7 The center of panel thermal conductivity of the fumed silica core provided by manufacturer B as function of the water content (2^0C-18^0C). The mean thermal conductivity increase rate up to 3.1% water content was 0.46(mW/mK)/1%.

H_2O [ML]	L [MW/MK]	DL [MW/MK]	$\%_{WT}$ H_2O	DL / $\%_{WT}$ H_2O
0	5.08	0	0	
1.15	5.27	0.19	0.353846154	0.536956522
2.25	5.485	0.405	0.692307692	0.585
3.25	5.66	0.58	1	0.58
4.25	5.85	0.77	1.307692308	0.588823529
5.25	5.98	0.9	1.615384615	0.557142857
6.25	6.075	0.995	1.923076923	0.5174
7.65	6.24	1.16	2.353846154	0.492810458
9.05	6.395	1.315	2.784615385	0.472237569
10.15	6.519	1.439	3.123076923	0.460763547

Table 2: The measured data of λ as function of the water content taken on core B at steady state conditions (20^0C-180^0C). The data points of the slope of the curve are shown in the far-right column.

8. Measuring the λvs Water Content Curve of the FS Core C

The same test procedure carried out on Core B was also performed on a 20mm thick core provided by manufacturer C. The density of this core under vacuum was 0.191g/cm^3.

As before, the panel was placed between the two plates of the λ machine along the entire duration of the test with 2^0C on the cold plate and 18^0C on the hot one.

The data describing the evolution of the water vapor pressure along the test duration is shown in Table 5 in the Annex below. As with core B, the time for reaching steady- state conditions also took much longer than core A, with a few days to one week required to reach steady-state. The λ data as function of the water content is shown in Table 3, and presented graphically in Figure 8, where the λvs Water content for core C is plotted.

Core C responded differently to the absorbed moisture compared to core A and core B:

a. Up to around 0.9% water content, the thermal conductivity rose almost twice as fast as Core A: 0.955mW/mK/1% compared to 0.49mW/mK/1%, also much faster than core B: 0.592mW/mK/1%.

b. The levelling off point of core C was substantially smaller (0.87%) than core A: (2%) and core B (1.31%). At a higher moisture content than the level off point,

the thermal conductivity of core C rose 3.93 times faster than core A: 0.521mW/mK/1% compared to 0.133mW/mK/1%.

c. The average slope of core C ({mW/mK}) was 2.18 times larger than for core A: 0.71mW/mK/1% compared to 0.321mW/mK/1%.

d. Core C was found to be much more sensitive to the absorbed moisture than both core A and core B.

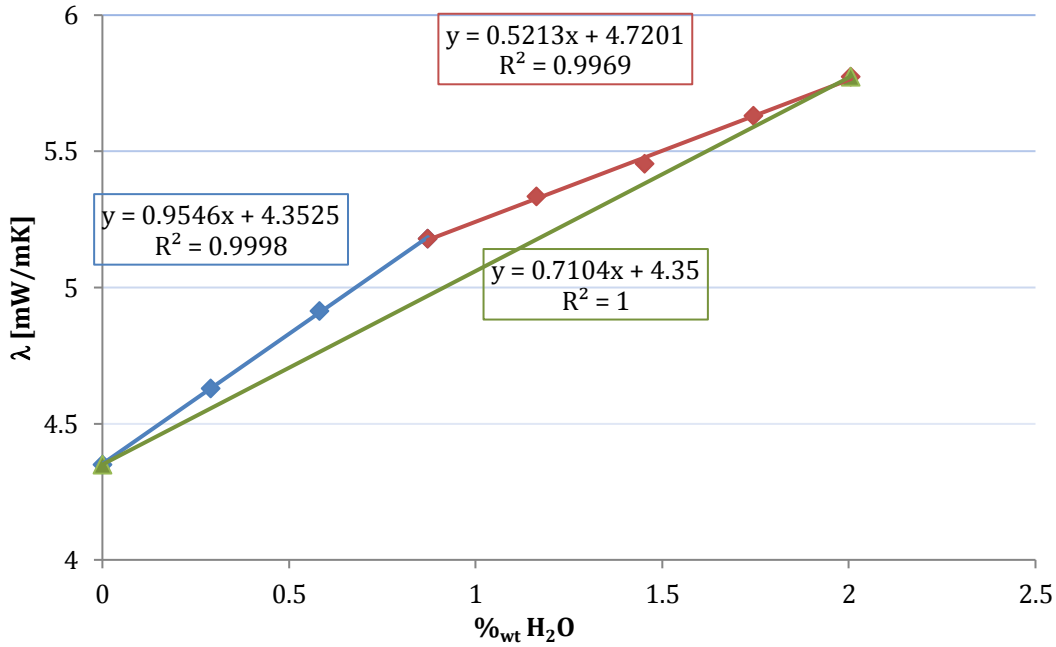

Figure.8: The center of panel thermal conductivity of the fumed silica core provided by manufacturer C as a function of the water content**.** The mean thermal conductivity increase rate up to 2% water content was 0.71(mW/mK)/1%.

H_2O [ml]	l [mW/mK]	Dl [mW/mK]	$\%_{wt}$ H_2O	Dl / $\%_{wt}$ H_2O
0	4.35	0	0	
1	4.63	0.28	0.290697674	0.9632
2	4.915	0.565	0.581395349	0.9718
3	5.18	0.83	0.872093023	0.951733333
4	5.334	0.984	1.162790698	0.84624
5	5.455	1.105	1.453488372	0.76024
6	5.63	1.28	1.744186047	0.733866667
6.9	5.775	1.425	2.005813953	0.710434783

Table 3: The measured data of λ as function of the water content taken on core C at steady-state conditions (2^0C-18^0C). The data points of the slope of the curve are shown in the far-right column.

Testing the performance of CaO desiccants

The goal of this test was to characterize the behavior of CaO desiccant (water vapor pressure and capacity) as a function of the absorbed water percentage.

a. Test Procedure

An mVIP system with a water measuring tube was connected to a fiberglass panel containing 10g of CaO desiccant. The mVIP also contained a capacitive pressure gauge (maximum pressure 10mbar). By opening the valve to the measuring tube, the desiccant drew measured amounts of water.

After adding a known measured amount of water into the internal volume of the panel, the system was kept at room temperature and the water vapor pressure inside the panel was continuously measured.

Table 4 and Figure 9 below describe the measured water vapor pressure as a function of the weight percentage of the water absorbed by the desiccant. The time to reach equilibrium pressure became longer and longer as the water content increased. Probably if we waited for longer than a few days after any dosage of water, the measured pressure could have been a bit lower.

Water Content (%)	Pressure (mbar)
10	0.365
15	0.66
20	0.71
28	0.86
38	2.6
45	P>10mbar

Table 4. The data points of close-to-equilibrium water vapor pressure at room temperature of CaO desiccant as function of the absorption percentage.

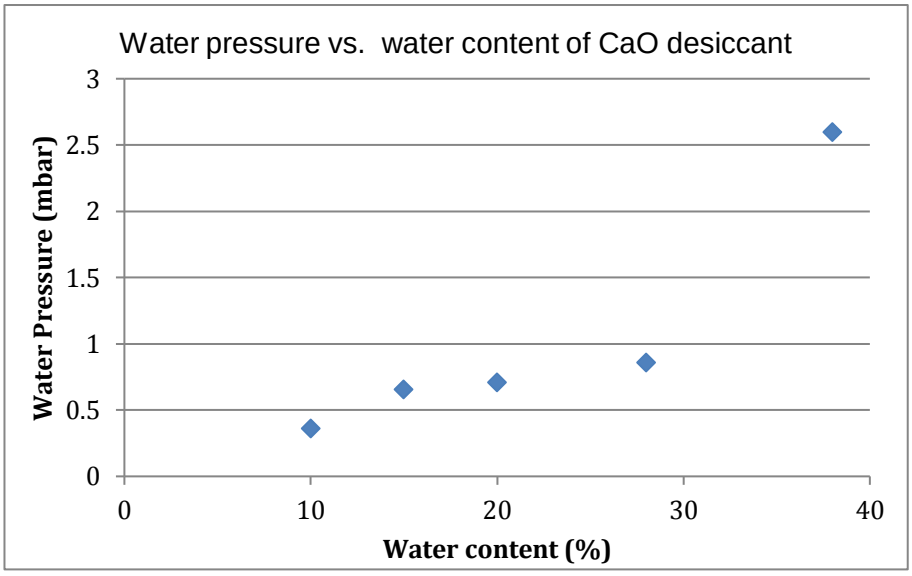

Figure 9: The close-to-equilibrium water vapor pressure inside FG panel with CaO desiccant as function of the weight percentage of absorbed water (room temperature).

b. Thermal Conductivity Measurements at Two Set-Up Conditions of the λ Machine

The thermal conductivity of the FG core with 38% absorbed moisture in the desiccant was measured at two sets of temperatures:

λ = 10.85mW/mK at 2^0C, 18^0C

λ = 11.95mW/mK at 10^0C, 35^0C

c. Conclusions Relating to the Measurements Made on CaO Desiccant

1. These preliminary results support the common opinion that the absorption capacity of CaO desiccants is around 30%.
2. It was found that the water vapor inside the FG panel was low up to 30%, and even at slightly higher water content levels.

Summary

1. A very accurate and easy to operate technique was developed for measuring the dependency of the thermal conductivity of fumed silica cores on absorbed water content.
2. This new technique, which is based on the mVIP system, is very cheap and can be easily adopted by any research or industrial laboratory.
3. By using the newly developed technique to investigate the response to the absorbed moisture of three fumed silica cores, it was found that each has a very different dependence of thermal conductivity to the absorbed moisture content. In addition, the time taken to reach steady-state for each data point differed for each core, from a few hours to up a week.
4. To minimize the time required to reach steady-state distribution of the moisture content, it is highly recommended to keep the panel between the plates of the λ machine for the entire test and to keep both temperatures constant.
5. For all three investigated fumed silica cores the slope $d\lambda/d$(%water content) was much steeper at low levels of water content, and more moderate at higher levels of water content.
6. The initial slopes, the turning points and the final slopes were all different for each of the three cores.
7. In view of the results of this short research, it is worth reviewing the assumption that all fumed silica cores respond identically to the percent of moisture content, as made in the CEN and the ISO standard draft documents for VIPs in building.
8. The system developed in this project can also be used to simply and accurately determine the absorption capacity of desiccants, as well as to measure the equilibrium water vapor pressure as a function of the absorption percent.

Recommendation

The technique developed in this project provides a very efficient tool to better predict the lifetime performance of fumed silica panels, and can help to achieve more accurate values for $\lambda_{Declared}$ compared to current methods. It is therefore recommended to integrate this new testing technique into all standards related to VIPs.

Signed:

Eddie Shufer and Dr. Yoash Carmi
Avery Dennison Hanita
Kibbutz Hanita, 2288500, Israel
Yoash.carmi@eu.averydennison.com

References

1. Schwab H. Heinemann U. Beck A. Ebert H-P. Fricke J. J. Thermal Environ. Bldg. Sci. 2005, 28, 293-317

Appendix

Core B. Evolution in time of the internal water vapor pressure as a function of water content.

Date	Time	ml of H_2O	P_{VIP} [mbar]	l [mw/mK]	
	09:50	10.15	28.5	5.08	valve open
	13:00	9	20	5.13	valve closed
9.10.16	14:45	9	8.85	5.125	
10.10.16	14:00	9	2.15	5.185	
	08:40	9	0.8	5.26	
13.10.16	16:20	9	0.7	5.27	
	07:00	9	0.4	5.27	
	07:45	9	28		valve open
	12:20	7.9	22		valve closed
	12:55	7.9	14		
	13:55	7.9	11.5		
	14:55	7.9	10	5.33	
18.10.16	15:55	7.9	8.85	5.345	
	06:00	7.9	4.75	5.41	
	11:35	7.9	4.25	5.425	
19.10.16	14:40	7.9	4	5.425	
	06:25	7.9	3.15	5.455	
20.10.16	13:50	7.9	3	5.455	
25.10.16	09:35	7.9	1.9	5.485	
	09:30	7.9	1.9	5.485	
	10:00	7.9	29.6		valve open
	13:40	6.9	20	5.515	valve closed
26.10.16	14:50	6.9	11.85	5.525	
	07:05	6.9	5.4	5.61	
27.10.16	15:35	6.9	4.6	5.63	
30.10.16	09:15	6.9	3.45	5.66	
	05:40	6.9	3.1	5.67	
	07:15	6.9	29.5		valve open
	11:55	5.9	20.5	5.75	valve closed
31.10.16	14:30	5.9	11.1	5.73	
	06:55	5.9	6.7	5.773	
1.11.16	15:50	5.9	6.35	5.8	
	07:00	5.9	5.5	5.815	
2.11.16	15:45	5.9	5	5.81	
3.11.16	11:20	5.9	4.6	5.815	

Date	Time	ml of H_2O	P_{VIP} [mbar]	l [mw/mK]	
	15:50	5.9	4.6	5.84	
	06:55	5.9	4	5.84	
	08:30	5.9	4.3	5.86	
	08:35	5.9	27.9		valve open
	13:45	4.9	21.5	5.93	valve closed
6.11.16	16:00	4.9	12.1	5.908	
	07:10	4.9	8	5.945	
7.11	16:00	4.9	7.15	5.965	
	07:00	4.9	Electric break		
8.11	14:00	4.9	6.7	5.983	
	07:35	4.9	6.1	5.975	
9.11	14:50	4.9	5.7	6.02	
10.11	15:10	4.9	5.7	5.98	
	10:20	4.9		5.98	valve open
15.11	14:35	3.9	21.35		valve closed
16.11	15:45	3.9	7.9	6.065	
22.11	08:15	3.9	6.1	6.072	
	06:05	3.9	6	6.075	
	07:15	3.9	27.7		valve open
23.11	14:45	2.5	18.2	6.113	valve closed
	06:00	2.5	9.75	6.14	
24.11	15:00	2.5	8.9	6.12	
	07:45	2.5	7.85	6.18	
27.11	15:35	2.5	7.5	6.19	
	06:15	2.5	7.8	6.22	
28.11	14:45	2.5	7.5	6.2	
	07:15	2.5	7.3	6.21	
	07:55	2.5	27.7		valve open
	15:00	1.15	23		valve closed
30.11	15:20	1.1	18.3	6.292	
1.12	15:20	1.1	9.2	6.31	
	06:25	1.1	8.5	6.385	
4.12	13:55	1.1	8.2	6.403	
5.12	13:00	1.1	8.3	6.395	

Table 5: Core B. Evolution in time of the internal water vapor pressure as function of the water content.

Core C. Evolution of time of the internal water vapor pressure as a function of water content.

		Full - 10.15 ml			
Date	**Time**	**Ml of h2o**	**Pvip [mbar]**	**□ [mw/mk]**	
25.1.17	07:10	10	>1	4.35	
	08:00		24.5		valve open
	12:00	9	18.5		valve closed
	13:00		7.8	4.45	
	14:00		6.7	4.473	
30.1.17	15:30		0.58	4.715	
31.1.17	13:00		0.3	4.63	
1.2.17	15:00		0.45	4.64	
5.2.17	06:30		0.45	4.58	
	08:50		0.46	4.6	
	09:10		30		valve open
	14:00		18.5		valve closed
	15:20	8	10.6	4.81	
6.2.17	06:30		8.6	4.85	
	12:00		7.3	4.915	
	15:30		7.5	4.95	
7.2.17	06:30		6.3	4.97	
	15:00		5.85	4.97	
8.2.17	06:30		5.5	4.967	
	12:30		5.5	4.971	
	15:30		5.5	4.97	
9.2.17	15:30		4.8	4.98	
12.2.17	18:00		4.6	4.98	
13.2.17	07:00		4.6	4.975	
	07:20				valve open
	10:20	7			valve closed
	17:00		9.6	5.08	
14.2.17	08:00		8.65	5.13	
	17:00		8.5	5.16	
15.2.17	13;30		8	5.18	
16.2.17	06:30		7.5	5.18	
	15:00		7.5	5.19	
19.2.17	08:00		7	5.19	
	08:00		28.3		valve open
	11:30	6			valve closed
	15;30		10.8	5.25	
20.2.17	07:30		10.3	5.26	
	15:30		10.15	5.28	
21.2.17	07:30		9.85	5.3	

		Full - 10.15 ml			
Date	**Time**	**Ml of h2o**	**Pvip [mbar]**	**□ [mw/mk]**	
	14:30		9.8	5.32	
22.2.17	06:30		9.6	5.33	
	15:30		9.6	5.35	
23.2.17	07:30		9.56	5.334	
	08:30		30		valve open
	13:00	5			valve closed
	15;30		12.8	5.4	
26.2.17	07:00		11	5.465	
	15:30		11	5.47	
27.2.17	12:00		10.85	5.455	
	15:00		10.9	5.458	
28.2.17	08:00		10.85	5.455	
	08:00				valve open
	12:30	4			valve closed
	16:00		12.45	5.49	
1.3.17	07:30		12	5.515	
	14:00		12.05	5.53	
2.3.17	08:00		11.9	5.575	
	15:30		11.8	5.56	
5.3.17	08:00		11.55	5.62	
	14:00		11.5	5.63	
12.3.17	09:00		10.95	5.65	valve open
	09:00	3.1			valve closed
	15:00				
13.3.17	07:00		13.8	5.75	
14.3.17	08:30		13.7	5.76	
	15:30		13.8	5.762	
15.3.17	09:30		13.8	5.775	

Table 6: Core C. Evolution of time of the internal water vapor pressure as function of the water content.